FINAL REPORT

ADVANCED NANOSCALE COATINGS WITH PLASMA SPRAY

ONR GRANT NUMBER: N00014-98-1-0420

Submitted To:

Dr. Lawrence Kabacoff
ONR Program Officer

Submitted by:

Oregon Graduate Institute of Science and Technology

Dr. David G. Atteridge
Principal Investigator

Co-Authors
Martin Becker, Graham A. Tewksbury, Milton Scholl

April 2000

REPORT DOCUMENTATION PAGE

Form Approved
OMB No. 0704-0188

1. AGENCY USE ONLY *(Leave Blank)*	2. REPORT DATE	3. REPORT TYPE AND DATES COVERED
	06/03/2001	Final Report: April 1, 1998 – September 30,1999

4. TITLE AND SUBTITLE
Advanced Nano-Scale Coatings With Plasma Spray

5. FUNDING NUMBERS
Grant #: N00014-98-1-0420
PR#: 98PR04561-00
99PR03291-00
99PR05860-00

6. AUTHORS
David G. Atteridge
Milton Scholl
Matin Becker, Graham Tewksbury

7. PERFORMING ORGANIZATION NAME(S) AND ADDRESS(ES)
Oregon Graduate Institute of Science and Technology
20000 NW Walker Road
Beaverton, OR 97006-8921

8. PERFORMING ORGANIZATION REPORT NUMBER

9. SPONSORING / MONITORING AGENCY NAME(S) AND ADDRESS(ES)
Office of Naval Research Seattle Regional Office
1107 NE 45th Street, Suite 350
Seattle, WA 98105-4631

10. SPONSORING / MONITORING AGENCY REPORT NUMBER

11. SUPPLEMENTARY NOTES

12a. DISTRIBUTION / AVAILABILITY STATEMENT
Distribution Statement A

12b. DISTRIBUTION CODE

13. ABSTRACT *(Maximum 200 words)*

The Oregon Graduate Institute was originally charged with assessing the potential of using plasma spraying techniques to produce thermal spray coatings consisting of tungsten carbide (WC) particles in a cobalt (Co) matrix (WC-Co). The WC particles of interest in this study were those with size on the nanometer scale embedded in a Co matrix. A secondary research charter developed as this program proceeded was the assessment of the feasibility of using cored wire filled with WE-Co powder as a feed-stock for both plasma spray and twin-wire-arc spray (TWAS) coating applications.

14. SUBJECT TERMS
High Energy Plasma Spray (HEPS), nanostructured, WC-in-

15. Number of Pages
32

16. PRICE CODE

17. SECURITY CLASSIFICATION OF REPORT	18. SECURITY CLASSIFICATION OF THIS PAGE	19. SECURITY CLASSIFICATION OF ABSTRACT	20. LIMITATION OF ABSTRACT
Unclassified	Unclassified	Unclassified	

PROGRAM OVERVIEW

* High energy plasma spray [HEPS] of "nanostructured" cermets has been found to yield consistently high quality coatings under a wide variety of spray parameters/conditions if readily sprayable powders are used.

*HEPS coating quality was found to be directly related to powder spray properties, i.e., powder flow characteristics and powder capture rate.

*Most WC-Co powder lots received from Nanodyne were found to exhibit very poor spray properties.

* HEPS has been shown to be capable of producing very high volume WC-in-Co coatings, namely powder with Co as low as 5 wt% has been successfully sprayed.

* Use of cored-wire feed-stock filled with "nanostructured" powder has been demonstrated to be feasible for both twin wire arc spray and HEPS.

* Use of twin wire arc spray of "nanostructured" cermets has been demonstrated to be feasible and to lead to unusually high bond strengths.

*SEM and TEM analysis of multiple Nanodyne-furnished powder revealed they contained sub-micron-sized WC particles versus the maximum 100 nanometer-sized particles expected.

*Only one out of six Nanodyne powder lots was found contained WC particles on the order of 20 to 100 nanometers in diameter, as determined by SEM and TEM assessment.

INTRODUCTION

The Oregon Graduate Institute (OGI) was originally charged with assessing the potential of using plasma spraying techniques to produce thermal spray coatings consisting of tungsten carbide (WC) particles in a cobalt (Co) matrix (WC-Co). The WC particles of interest in this study were those with size on the nanometer scale embedded in a Co matrix. A secondary research charter developed as this program proceeded was the assessment of the feasibility of using cored wire filled with WC-Co powder as a feed-stock for both plasma spray and twin-wire-arc spray (TWAS) coating applications. This reports highlights research for the program funded through September 31, 1999.

The following sections cover a figure -of-merit analysis of thermal spray powders containing nanometer scale WC particles, WC-Co powder plasma spraying results, results obtained plasma spraying and twin-arc spraying with WC-Co powder cored wires, and the results of a study characterizing the WC-Co powders used in this research program.

FIGURE-OF-MERIT ANALYSIS OF FEASIBILITY

Nanoscale cermets such as the tungsten carbide cobalt (WC-Co) for thermal spray differ from conventional cermets. Conventional WC-Co thermal spray powders typically have a small numbers of tungsten carbide particles within the cobalt matrix, the tungsten carbide particles themselves being on the order of micrometers in scale in a powder particle which ranges from 20 to 75 μm in diameter. On the other hand, nanoscale WC-Co powders have a large number of very small tungsten carbide particles (nanometer scale) in a cobalt matrix with an equivalent powder particle size (20 to 75 μm in diameter).

Due to the quite different nature of each type of particles, the multi-phase melting and flow characteristics are also quite different. If all the cobalt melts, then the nanoscale droplet may have a much more fluid characteristic than the corresponding conventional powder, i.e. one with the same volume fraction of WC and cobalt. That greater fluidity can result in more effective spreading on contact with the surface. The nanoscale powder thus has the potential for highly uniform coatings. This fluidity and

uniformity may not be achieved fully if the droplet were not to experience complete melting. There may be sufficient melting to promote adhesion without obtaining uniform spreading. A coating may thus be applied successfully without gaining all the benefits associated with nanoscale grain sizes.

Accordingly, the following analysis provides development of a figure of merit relating the time needed to completely melt a droplet relative to the time the droplet is in a heating environment. It will be seen that for high-energy plasma heating, the figure of merit is such that complete melting is to be expected. This is consistent with the observations to date that coatings deposited by high-energy plasma tend to be uniform and of high quality under a very wide range of deposition conditions.

For cored wire, whether using twin wire arc spray or using cored wire feed in a high-energy plasma system, complete melting must occur. This is because it takes melting to have liquid break off from the wire. In the plasma system, there may be more opportunity for superheating, but in either case, melting would be complete.

One figure of merit discussed here is only with regard to heating and completeness of melting. Providing substantially more thermal energy than is needed for melting can lead to other effects, particularly to decarburization. The significance of a moderate degree of decarburization for nanoscale powders is not well established. A separate figure of merit analysis will be provided for decarburization. Since both melting and decarburization take place, it is of interest to understand how both processes evolve together. The ratio of decarburization to melting is modeled approximately. Interesting observations on the dependence of this ratio on temperature of the gas stream are noted. Since velocity is a parameter that may be varied in spraying, the influence of velocity is examined. Here it is noted that velocity affects both melting and decarburization, explaining some results reported during the ONR program.

Heating to the Melting Point

A simple lumped parameter analysis will be used to provide an initial assessment of relative importance of various factors. Consider first the heating of a particle from a starting temperature to the temperature at which it melts or at which a constituent (e.g. cobalt in a WC-Co particle) melts. The governing equation is:

$$pcV\frac{dT}{dt} = \lambda A(T\infty - T_0)$$

where p is the density, c the heat capacity, V the volume of the particle, λ the heat transfer coefficient, A the cross-section area of the particle, and T_o the initial temperature and T_∞ the environment temperature.

If the properties are independent of temperature (or if effective average properties can be used), then the equation can be integrated to yield:

$$\frac{T\infty - T_M}{T\infty - T_0} = \exp-\frac{A\lambda}{cVp}t_H$$

The heating time to melting may then be expressed as:

$$t_H = \frac{1}{3}\frac{pcR}{\lambda}\ln\frac{T\infty - T_0}{T\infty - T_M}$$

where R is the radius of the particle. If the gas temperature is much greater than either the starting or melting temperatures (a good approximation for plasma), the logarithms can be expanded to yield:

$$t_H \approx \frac{1}{3}\frac{pcR}{\lambda}\frac{T_M - T_0}{T\infty}$$

Examination of the expression for heating time indicates that the heating time should be much shorter for plasma and high energy plasma (gas temperatures about 15,000°C) relative to HVOF (gas temperatures about 3000°C). For convenience, the melting time can be expressed in terms of diffusivity α and Nusselt number Nu:

$$t_H \approx \frac{2}{3}\frac{R^2}{\alpha Nu}\frac{T_M - T_0}{T\infty}$$

Melting

In a lumped parameter model, the cermet mixture will heat up uniformly until the melting temperature of the matrix material (typically cobalt) is reached. Then, all material will remain at the melting temperature while the matrix material undergoes melting. Dynamically, the fraction of the matrix material that is liquid will vary from zero to one according to

$$pcVfh_M\frac{dp}{dt} = \lambda A(T\infty - T_M)$$

where f is the fraction to melt and h_M is the latent heat of melting. This equation can be integrated. The melting time corresponds to the condition when the liquid fraction is one. The melting time is given by:

$$t_M = \frac{pcVfh_M R}{3\lambda(T\infty - T_M)}$$

Note that the ratio of volume to area has been replaced by one-third the radius. The figure of merit will be defined as the ratio of residence and melting times:

$$FOM_M = \frac{t_R}{t_M}$$

If the residence time is longer than the melting time, full melting takes place and the figure of merit exceeds one. Note that while melting is deemed desirable, a figure of merit far in excess of one may have disadvantages. While some superheating may be desirable (to avoid resolidification before impact), additional heating may lead to additional decarburization without providing any additional direct benefit.

Estimation of Figure of Merit

The following data will be used for estimating purposes:

Density $\rho = 890$ Latent heat $h_M = 3x10^5$

Radius $R = 25x10^{-6}$ Cobalt fraction $f = .1$

Heat transfer coefficient $\lambda \cong k/R = .1/25x10^{-6}$ (Nu=2)

Diffusivity $\alpha = 25x10^{-6}$

For high energy plasma, temperature difference = 13,000°

t_R = .04msec t_M = .04msec

Given these quantities for HEPS the typical value of the figure of merit is one and therefore melting should be complete. Note that this assumes the particles enter the core of the plasma plume, which may or may not happen.

Decarburization

For the purposes of initial inquiry, decarburization will be represented by a rate equation of the form:

$$\frac{dC}{dt} = -KC$$

The rate of carbon loss dC/dt, is assumed proportional to the carbon concentration, C. The coefficient K is assumed to depend on temperature according to the Arrhenius formula:

$$K = K_0 \exp - Q / RT)$$

At the outset, we can assume the decarburization rate to depend on the initial carbon content, and integrate to yield a decarburizing time

$$t_C = \frac{C_0 - C}{KC_0}$$

How much decarburization takes place will depend on how long the particle remains in the heating environment. If decarburization is considered to be something to avoid, then we may define a decarburization figure of merit that relates the decarburizing time to the residence time:

$$\mathrm{FOM_C} = \frac{\mathrm{t_C}}{\mathrm{t_R}}$$

If the time needed to cause an amount of decarburization that is deemed detrimental to coating quality is substantially less than the residence time, then the figure of merit is much less than one and serious decarburization takes place. It the decarburizing time is much greater than the residence time, then decarburization should not be a problem.

Melting and Decarburization

Melting and decarburization have been examined separately. Let us now consider these processes taking place simultaneously. From the section on melting, the fraction of matrix material that has melted in a time t can be obtained as:

$$\mathrm{p} = \frac{3\lambda(\mathrm{T_g} - \mathrm{T_M})}{\rho f h_{\mathrm{M}} R} t$$

During the same time, the fractional decarburization is:

$$\mathrm{c} = \frac{\mathrm{C_0} - \mathrm{C}}{C_0} = K_0 \exp -(Q / RT_M)t$$

The ratio of decarburization to melting is then:

$$\frac{c}{p} = \frac{K_0 \exp(-Q/RT_M)}{3\lambda(T_g - T_M)} \rho f h_M R$$

During the melting process, decarburization depends on the melting temperature, while melting depends on the difference between gas and melting temperatures. Roughly speaking, decarburization associated with a given degree of melting is reduced if the gas temperature is increased. In other words, for a given total heat input (to achieve a specified degree of melting), decarburization is reduced by delivering the heat more intensely for a shorter period of time.

The implication of this observation is that during the melting process itself, high temperature processes like plasma should yield less decarburization than typically expected even though plasma processes are generally thought of as more decarburizing because they frequently deliver more heat than is necessary for melting, producing superheat and additional decarburization. Adjustment of process parameters, like the location of external feed entry to the gas stream, may thus reduce decarburization by reducing unnecessary heating.

Influence of Velocity

It is possible to vary velocities by adjustment of gas flow rates for given input power and by use of nozzle attachments. Both heat and mass transfer are affected by velocity. The Nusselt number (dimensionless heat transfer coefficient) has been represented by

$$Nu = 2 + .66 Re^{.5} Pr^{.33}$$

where **Re** is the Reynolds number and **Pr** the Prandtl number.

Velocity is included in the Reynolds number, so heat transfer should increase the square root of velocity. Since mass transfer is based on directly analogous phenomena, mass transfer relations tend to be similar to heat transfer relations, with the Nusselt

number replaced by the Sherwood number and the Prandtl number replaced by the Schmidt number. Velocity dependence through the Reynolds number tends to be the same.

It has been observed in the ONR nanoscale program that an HVOF system with a nozzle attachment produced far better coatings than one without the attachment, but also produced substantially more decarburization. One possible explanation is that the system without the nozzle produced incomplete melting, and consequently poor coatings. Enhanced heat transfer obtained with the nozzle could thus have led to sufficient melting to achieve good coatings. Intrinsically associated with heat transfer increase is a mass transfer increase, i.e. increased decarburization. The essence of this section is to note that important processes and phenomena are interdependent.

HIGH ENERGY PLASMA SPRAYING USING WC-Co POWDER WITH MICROMETER, SUB-MICROMETER, AND NANOMETER- SCALE TUNGSTEN CARBIDE

The high energy plasma spraying was carried out at the Oregon Graduate Institute using a 200 KW Plazjet plasma spraying system. This system operates from 200 to 500 Volts and 100 to 500 amperes, with gas flows from 100 slpm nitrogen to over 400 slpm nitrogen. Nitrogen/hydrogen mixtures can also be used at ratios over 1:1. The system is capable of spraying both wire feedstock from 0.8 mm to 3.2 mm diameter or powder feedstock from 10 micrometers to over 150 micrometers in size; or both may be used simultaneously.

High energy plasma spray (HEPS) coatings were made using micron-, submicron-, and nanometer-scale tungsten carbide in a cobalt matrix as powder feed stock. The powders were sprayed in the as-received condition, without further processing. Cobalt matrix composition varied from 6 to 15 wt%.

The thermal spray coatings were deposited on carbon steel substrates grit-blasted just previous to spray coating. Several spray parameter sets were run for each

material. Subsequent analysis and testing included optical, SEM, TEM, and ASTM G65-94 dry-sand-rubber-wheel wear testing.

Several batches of Nanodyne-produced WC-Co powder were sprayed as a function of stand-off distance, gas composition and pressure. Coatings with a wide variation in quality were produced, with the quality dependent on the "sprayability" of the as-received powder. One of the major problems was that the dry flowability of the powders was quite poor. Subsequent analysis (detailed later in this report) indicates that the majority of the Nanodyne powders exhibited a very wide size distribution, with a large amount of fines (micrometer and sub-micrometer particle fragments) as well as fractured particles. It is felt that the large amount of fines inhibited the material from flowing smoothly, or at all, through the HEPS powder feeding system. In addition, it is felt that the wide size distribution made it essentially impossible to obtain reasonable particle capture rates, as only a reasonably small segment of the given powder distribution would be "suitable" to form a (high quality) coating for a given HEPS parameter set. Thus, even when OGI was able to find a method to overcome the poor flow properties of the powders, the resultant powder capture rate was insufficient to yield a reasonable thickness/quality coating.

OGI's powder flow problems lead it to modify its powder feed system. Namely, the system was changed from a dual powder input system to a single powder input system. The tubing used to feed the powder input system was also increased in size. These powder feed modifications allowed previously unsprayable powders to now be sprayed, but yielded such poor particle capture rates that the resultant coatings were nominally of un-acceptable quality. Thus, the powder feeding system was changed back to the two nozzle powder feed configuration.

Sprayable Nanodyne WC-Co powders were found to yield good coatings over a range of spray distances from 100 to 200mm, a very wide spray distance tolerance envelope. These coatings were also found to yield acceptable coating quality over a wider range of gas flow and mixture parameters than found for commercially- available micrometer-sized WC-Co powders. Commercially available micrometer-size WC-Co powder with variable cobalt composition previously sprayed were used for this

comparison. Cobalt matrix content for the micrometer-sized material varied from 12 to 17 wt%. Figures 1 and 2 show typical photomicrographs of a WC-Co coatings with submicrometer scale WC (Figure 1) and micrometer scale WC (Figure 2).

Knoop hardness values over 1000 were found for the WC-Co coatings fabricated using Nanodyne powders, while values under 1000 were found for the micrometer-scale WC-Co coatings. Selected area Knoop harness values up to 1100 were found for the original 12% WC-Co powder while values up to 1300 have been measured for the recently sprayed 6% WC-Co specimens. The Nanodyne WC-Co coatings were found to have less variation due to spray parameter changes than the micrometer-scale WC-Co coatings. For instance, 15% Co coatings were found to be acceptable, from a wear and hardness standpoint, with a change of spray stand-off distance of 10 cm. The high-quality Nanodyne WC-Co coatings exhibited a decrease in wear rate in comparison to the micrometer-scale WC-Co coatings. Coating porosity was found to be less in the Nanodyne powder versus the micrometer scale WC-Co coatings. Optical and SEM analysis showed porosity volume fraction values ranging from 0 to 6 percent for the various types of coatings, depending on processing parameters and Co matrix percent.

TWIN WIRE ARC AND HIGH ENERGY PLASMA SPRAY COATING USING NANOMETER-SCALE WC-CO POWDER FILLED CORED WIRE

The feasibility of producing cored wire filled with WC-Co powder was demonstrated by having a metal-sheathed wire made filled with WC-Co powder. The feasibility of using this core-wire feed-stock for thermal spray coatings was also demonstrated. Thermal spray coatings were made using Nanodyne-furnished powder-filled cored wire. Three different cored wires were produced by Devasco using two different wire sheath materials. The sheath materials were commercially pure nickel and 430 stainless steel and were filled with one of two Nanodyne-produced WC-Co powder compositions, either 6% or 15 percent wt% Co powders. Both 6 and 15 wt% WC-Co powders were used with the nickel sheathed wire, while only the 6 wt% WC-Co was used with the 430 stainless steel sheath material. The cored wire diameter and sheath thickness combined to yield a sheath material-to-powder 50-50 volume percent ratio. The cored wires were used as feed stock for producing coatings using twin wire

arc spray (TWAS) and high energy plasma spray (HEPS). The TWAS was carried out at the Puget Sound Naval Shipyard (PSNS) while the HEPS was carried out at the Oregon Graduate Institute.

Twin wire arc spraying feasibility for the nano-WC-Co cored-wire feedstocks was carried out at the Puget Sound Naval Shipyard (PSNS) using a Thermion system. Air pressure was held constant at 100 psi while current was held constant at 200 amps. Initial voltage settings were determined using a Devasco-produced high-manganese cored-wire of similar size due to the small quantities of the wire containing the nanometer-scale WC. None of the cored-wires contained fluxing agents as found in cored welding wire. The experimental spraying parameters varied from 25 to 35 volts, but were not optimized due to the small amount of material available. The core-wire was found to be sprayable at lower voltages than solid wire feedstock.

The performance of the coared wire was also evaluated with OGI's high-energy-plasma spray system. As with the TWAS, parameters were assessed with the high-manganese cored-wire before using the nanometer scale WC-containing wire. Nominal spraying parameters were 5 cfm nitrogen, up to 2 cfm hydrogen, 400 volts and 400 amps.

All three wires (Ni+WC-Co, 430+WC-Co, High Mn) were used to produce coatings with the TWAS, while only the nickel sheathed wires were used to produce coatings with the HEPS due to the limited amount of 430 stainless steel wire procured. The thermal spray coatings were deposited on carbon steel substrates grit-blasted just previous to spray coating. Several spray parameter sets were run for each thermal spray technique, although parameter optimization was not possible due to the limited amount of cored wire procured for this feasibility study. Subsequent analysis and testing included optical, SEM, dry-sand-rubber-wheel abrasive wear testing, and adhesion strength testing.

Adhesion strength for the TWAS coatings was measured at PSNS. The TWAS coating adhesion values were found to be very high. Adhesion strength for the TWAS coatings was also found to improve with increasing WC content. The adhesion values for the nickel-sheathed TWAS coatings were found to be 9.2 ksi for the 15%Co coating

and 10.4 ksi for the 6%Co coatings, with the higher values being a lower bound as the test failures took place in the epoxy versus the coating or coating/substrate interface. In fact, the Nickel+WC-6%Co TWAS coating adhesion results were found to be the highest thermal spray coating adhesion results to date by PSNS. The 430 stainless steel sheath coating exhibited an adhesion strength of 7.6ksi.

Wear resistance, hardness and porosity were found to be comparable between spray techniques. Wear resistance was found to improve with increasing WC content, however, the best dry-sand-rubber-wheel wear results were still "high" wear rates compared to the WC-Co coating results we are getting with much higher WC volume fractions. This is not unexpected for these composition materials; sliding wear rates may prove to be much better for the nickel matrix material. This material is obviously not an optimum wear material, which is not surprising as its main benefit to the Navy is its corrosion resistance. The 6%Co 430 stainless steel-based coating wear rate was superior to that of the 6%Co Ni-based coating.

Nickel-based coating hardness was found to increase as the WC content was increased. Comparable Nickel+WC-6%Co coating hardness was found for the TWAS and HEPS coatings, while the Nickel+WC-15% Co HEPS coating was found to be harder than the TWAS coating. Optical and SEM analysis showed porosity values for the TWAS coatings in the range of 3% for the nicekl-based coatings and 7% for the 430 stainless steel coatings. The porosity of the HEPS coatings was found to be somewhat higher than that of the TWAS coatings. SEM analysis showed the presence of WC, and that the distribution of the WC-Co in the nickel “matrix”was non-uniform.

ASSESSMENT OF TUNGSTEN CARBIDE-COBALT POWDERS

The Oregon Graduate Institute of Science and Technology (OGI) has received a number of WC-Co powders reported to contain either conventional micrometer-scale or nanometer-scale tungsten carbide (WC) particles embedded in a cobalt matrix. The WC-Co powders were purchased on the open market or received from the Office of Naval Research (ONR). The powder suppliers included Sulzer-Metco, Osram-Sylvania, Nanodyne, and Inframat. OGI purchased its first lot of Nanodyne powder prior to the inititation of this ONR program. Multiple additional Nanodyne powder lots were

received by OGI over the duration of this ONR funded program. A listing of suppliers, product lot numbers, composition, and powder receiving dates are given in Table I. The Sultzer-Metco powders were expected to have micrometer-scale WC particles embedded in the Co matrix. The Osram-Sylvania powder was expected to have sub-micron-scale WC particles while the Nanodyne and Inframat powders were expected to have nanometer-scale WC particles. All powders were expected to be sprayable by the Oregon Graduate Institute (OGI) high energy plasma spray (HEPS) system.

This section presents an overview of the spray-oriented properties of the various powder lots received by OGI as well as a discussion of their associated WC particle characteristics. The powder properties/characteristics covered herein include an assessment of the thermal spray powder particle size distribution; microstructure and topography of powder particles; and an assessment of WC particle size distribution.

Characteristics of the Thermal Spray Powders

The external and internal characteristics of the powders received by OGI for thermal spraying are described in this section. An overview of the various powder characteristics is given first; followed by a section describing each individual powder. In general the powders could be characterized by conventional powders (shown in Figure 3), 'good' powders with nanoscale WC (shown in Figure 4), and 'poor' powders with nanoscale WC (shown in Figure 5). The conventional and 'good' powders were those which had uniform particle morphologies and few fines, while in the 'poor' powders fines and particle fragments predominated.

The first powder characteristic assessed was that of "flowability". This qualitative property is critically important to the thermal spraying operation, as coatings can not be produced efficiently if a powder doesn't flow well. Generic ranking of flowability of these powders was that the Sulzer-Metco, Osram-Sylvania, Inframat, and the first and last batch of the Nanodyne powder flowed reasonably well. The intermediate Nanodyne powder batches did not flow or flowed poorly (Table II).

Further investigation into the differences in powder flow characteristics revealed a wide difference in spray powder size distribution and spray powder particle morphology. The Sulzer-Metco, Osram-Sylvania, Inframat, and last lot of the Nanodyne powder consisted of nominally spherical spray particles with a reasonably

narrow size distribution. Of the Nanodyne materials, all but the last lot exhibited a combination of spherical powder particles, fractured spherical spray particles and fragments, and micrometer to sub-micrometer fines as debris from damaged/crushed particles, and, thus exhibited a wide particle size distribution (Table II).

The WC grain size distribution internal to the individual powder particles for the various powder lots was also assessed using a conbinamtion of scanning electron microscopy and transmission electron microscopy. The Sutzer-Metco WC particles were found to be in the micrometer-scale. The Osram-Sylvania lot, several of the Nanodyne powder lots, and the Inframat lot was found to contain submicrometer-scale WC particles. Only one of the ONR-programmatic Nanodyne lots assessed was found to contain nanometer-scale WC particles as detailed in Table III.

Characterization of Individual Powder Lots

Selected lots of WC-Co powder received by OGI were analyzed in depth. All were subjected to SEM analysis; some were subjected to TEM analysis also. Thermal spray powder size and distribution, as well as external spray particle size morphology were assessed by SEM on the as-received powder. As-received powder samples were then mounted and metallographically polished to allow SEM assessment of spray particle internal structure and WC particle size and distribution. The WC particle size and distribution was assessed in the back-scattered and secondary electron imaging modes.

Particles on the order of 100 nanometers and above were readily defined by high resolution SEM backscatter work. WC particles less than 20 nanometers were discernable, but quantitative size/distribution assessment was not possible due to the low resolutions of the images. The SEM analysis was supplemented by TEM analysis for the powders exhibiting WC particle sizes below 50 nanometers in the SEM analysis. TEM specimen preparation consisted of crushing the powder into a very fine dust through the use of a mortar and pestle, suspending the resultant dust particles in a nital solution using an ultrasonic cleaner, and then capturing the dust particles on a TEM grid. Transmission mode electron microscopy was then used for subsequent WC particle analysis. The results of these examination techniques are presented below for the various WC-Co powder lots.

Sulzer-Metco Powders

The Sulzer-Metco powders consisted of solid, nominally spherical or oblong particles with a relatively tight particle size range for the majority of the particles in the 10 to 70 μm size range with essentially no "fines", as assessed by SEM observations at OGI. The SM-1 (12%Co) spray powder exhibited spherical spray particles with an approximate particle size range of 10 to 70 μm, as determined by the SEM visual assessment technique. The results of a particle distribution scan done using a Lecotron-LT100 yielded a 8 to 102 μm range. This scan was done by taking the spray powder and mixing it with a liquid flowing agent (water) and then flowing the suspended particles past a laser particle size discrimination detector. The average particle diameter was determine to be 30.4 μm. The SM-2 (17%Co) spray powder exhibited mostly oblong particles with a few spherical particles mixed in. An approximate range of 10 to 60 microns was estimated for this powder lot by the SEM method. The Lecotron yielded a size range of 9 to 140 μm with an average diameter of 34.8 μm. The SM-3 (12%Co) spray powder exhibited a majority of oblong spray particles with a particle size range between 30 to 70 μm, as estimated by the SEM visual technique. All three powders flowed readily. Note that the SEM spray particle size range visual estimation technique underestimated the actual size range, but contained over 95 percent of the particle range for the SM-1 lot and over 90 percent of the particles for the SM-2 lot. Thus, visual particle range estimation appears to be reasonable for particle lots consisting of particles with a reasonable tight size range and little or no fines.

The spray powder spherical/oblong particle surface of the Sultzer-Metco powder lots exhibited large, prismatic micrometer-scale WC particles embedded in the cobalt matrix. The SM-3 lot was examined in cross-section and was found to exhibit 1,000 to 2,000 nanometer (1-2 μm) WC particles. It was also found to be essentially solid.

Nanodyne Powders

The first five nano-powder Lots from Nanodyne nominally consisted of low density fractured powder particles and particle flakes from the fracture of larger particles which generally yielded a large amount of fines. The sixth Nanodyne Lot (Lot N-6) consisted of relatively dense spherical powders with few fines.

The Lot N-1 (12%Co) Nanodyne powder consisted of mainly undamaged particles with few small flake particles. Lot N-1had a nominal size range of 10 to 100

μm by SEM analysis. A Lecotrac particle distribution assessment indicates a particle size range from 0.8 to 210 μm with ~26 volume percent below 10 μm and ~3 volume percent above 100 μm. Thus the SEM visual estimation technique apprears to be reasonable in the upper limit side, but grossly underestimates the lower particle size region. The mean particle diameter was found to be 26.5 μm. The spray particles appeared to be hollow spherical balls with the possibility of small fractured particle debris within the fracture hollow spheres. This batch of powder readily flowed. Neither powder particle cross-sections or WC particle size was assessed for this lot of powder.

The Lot N-2 (15%Co) Nanodyne powder exhibited a nominal particle size range from 2 to 150 μm, with a large amount of fines. The particles appeared to consist of multiple spherical shells within spherical particles, resulting in a low-density, "filled" spherical particle. This powder had poor flow properties. Spray particle cross-sectional analysis revealed that the majority of spray particles appeared to be solid particles of varied shape, which included spherical, oblong and random-shaped particles. A thin outer skin of the solid particles appeared to have a higher density of WC particles than the interior. Thin-wall and thick-walled spheres, some filled with small particles and/or debris, were also found, along with multi-shelled spherical particles. The fines included small individual (solid) particles as well as particle fragments. Powder particle fragments are made up of solid particle fragments as well as thin-walled particle fragments. The WC particle size was found to vary between 200 to 500 nanometers (0.2-0.5 μm).

Lot N-3 (6%Co) Nanodyne powder exhibited a nominal particle size range from 2 to 150 μm, again with a large amount of fines. The particles appeared to consist of thin-walled spherical particles with a porous internal structure. The fines appeared to be fragments of larger, thin-walled particles. This powder had poor flow properties. Powder particle cross-sectional analysis revealed that the spherical particles varied from thin-walled spheres to thick-walled spheres to "solid" spheres, with some of the thin-walled spheres being filled with a porous internal structure. Thin/thick-walled spheres were also found to contain particles debris. The majority of the fines appeared to be made up of fractured thin-walled particles, as observed above. The previously observed "solid" particles appear to be thin-walled particles filled with particle debris. The WC particle size was found to vary between 200 to 1,000 nanometers (0.2-1 μm).

Lot N-4 (15%Co) Nanodyne powder consisted of spherical particles ranging in size from 5 to 300 microns with a high percentage of fines. The particles appeared to have a porous, foam-like, interior. This lot had very poor flow characteristics. Cross-sectional analysis of the powder particles revealed interior morphologies that ranged from "solid" to thick-walled particles, with the majority appearing to be solid particles. Thin/thick-walled particles filled with small particles and/or debris were also found. High-magnification examination of the solid particles revealed that these were actually porous. WC particles sizes were found to vary from 20 to 100 nanometers (0.02-0.1 μm).

Lot N-5 (5%Co) Nanodyne powder consisted of the same general size and shape spray particles as Nanodyne Lot N-4. Lot N-5 had a nominal range of particles sizes from 2 to 250 μm and consisted of a mixture of flakes and spherical particles, with a very high percentage of flakes. The broken spherical particles appear to be low density and highly porous. This powder had very poor flow characteristics. Powder particle cross-sectional analysis revealed that the vast majority of the spherical particles were very thin-walled with a few thick-walled particles mixed in. The previously observed "solid" particles appear to be thin-to-thick-walled particles filled with small paricles and/or particle debris. The WC particle size was found to vary between 200 to 1,500 nanometers (0.2-1.5 μm).

The Lot N-6 (12%Co) Nanodyne powder was separated into two size cuts prior to being sent to OGI. The larger particle size cut (>45 μm or +325 mesh cut) was essentially a "plasma" cut. The smaller particle size cut (all that wasn't in the larger sized cut) was a "HVOF" cut, plus fines. Both size cuts flowed reasonably well. The plasma cut powder was found to contain particles ranging from 20 μm to 100 μm while the HVOF cut contained particles ranging from 10 μm to 50 μm. The presence of particles smaller than 45 μm in the plasma cut is consistent with Rigney's observation that the Nanodyne powders tend to continuously produce small particle fragments with continued handling.

Both N-6 Lots of the as-received powder particles were mounted and polished part-way through in order to allow assessment of powder particle packing and original WC particle size. It was found that these as-received powders contained very few broken particles with the majority of particles being porous and containing a

reasonable amount of void spaces. Variable walled spherical particles were also present. Wall thickness was found to vary from very thin to very thick. It is assumed that the thin-walled particles continue to fragment with handling. Multi-layered spheres were found as well as thin-walled spheres that were filled with small particles and/or debris. The vast majority of the WC particles were 300 to 500 nanometers in size (0.3-0.5 μm).

Inframant Powder

The Inframat powder was actually a re-constituted Nanodyne power. The original Nanodyne powder was found to be unsprayable and was subsequently sent to Inframat for re-constitution in hopes of yielding a sprayable powder. The Inframat powder was separated into two size cuts prior to shipping to OGI, with OGI only receiving powder from the "fines" cut. The Inframat Lot I-1 powder was much more like the conventional powders in that it had a relatively narrow particle size distribution with only a small amount of flakes, except that the powder size was much smaller, and was found to flow well. The powder particle size appears to vary from 2 to 50 μm with essentially no flakes and the particles appeared to be solid. The Inframat as-received powder was mounted and polished part-way through in order to allow assessment of spray particle packing and original WC particle size. Cross-sectional analysis revealed that the spray particles exhibited a porous internal structure combined with minor to major pores. This powder also contained WC particles which ranged in size from 100 to 300 nanometers (0.1-0.3 μm).

Osram-Sylvania Powders

The Osram-Sylvania spray particles were spherical in shape and had a relatively narrow particle size distribution with only a small amount of flakes, with a spray powder size of 10 to 70 μm. These spherical spray particles appear to be solid and the powder flowed well. The Osram-Sylvania as-received powder was also mounted and polished part-way through in order to allow assessment of spray particle packing and original WC particle size. Cross-sectional analysis revealed that the spray particles contained very small pores with an occasional large pore. The powder particles were found to contain WC particles in the size range of 200 to 1,200 nanometers (0.2-1.2 μm).

DISCUSSION

Thermally sprayable powders need to exhibit a minimum of two major characteristics. The first is "flowability" and the second is a narrow size distribution range centered around a specific average size. A wide particle distribution on either side of a given parameter set's optimum particle size will result in a low particle capture rate and a poor quality coating. Particles (much) larger than the optimum will not be (completely) melted and simply bounce off the substrate; particles (much) smaller than the optimum will be vaporized. The Sultzer-Metco and Osram-Sylvania powder lots were expected to exhibit both of these desired properties as they were specifically produced as thermally-sprayable powders, and, indeed, all lots from these suppliers exhibited these two properties.

It was hoped that the Nanodyne powder lots would be thermally-sprayable, but, as they were not specifically fabricated as thermally-sprayable powders, this needed to be determined on a lot-by-lot basis. The Nanodyne powder lots were actually produced for the sintering industry. Here they are interested in easily friable powder particles, as they subsequently grind them into smaller particles prior to their sintering operation, versus the desire for robust particles in the thermal spray industry. A tight particle size distribution is of no concern to the sintering industry; as long as the particle is easily crushable the powder is acceptable to the sintering industry.

Study of the Nanodyne powders immediately reveled that the majority of the powder lots contained too large a particle size distribution to be effectively thermally-sprayed. It was also found that a combination of the wide size distribution and spray particle morphology, and, in particular, the large amount of fines, resulted in low flowability characteristics. The majority of the powder lots would rather clump than flow. Only the N-1 and N-6 powder lots exhibited acceptable flow properties. The Lot N-6 material actually had a continuous, though porous, structure throughout the particle interior versus spheres made up of single or multiple thin/thick walled spheres, as was the first five Nanodyne lots. The above analysis indicates that all (multi) shell Nanodyne powder lots were too friable to be used successfully as thermal spray powders. The Inframat powder lot was actually a re-constituted Nanodyne powder lot. The re-constitution process produced spherical, robust potentially-thermally-sprayable powder.

It was assumed that each supplier's powder contained a distinct size distribution of WC particles. It was expected that the powder would fall into three distinct ranges of WC particle sizes ranges, namely, micron size particles (1,000+ nanometer size), submicron sized particles (200 to 600 nanometers), and nanometer sized particles (less than 100 nanometers).

The WC particles contained in the commercial thermal spray material were found to be in the size range expected. The Sulzer-Metco exhibited micron-sized WC particles while the Osram-Sylvania powder exhibited submicron-sized particles. However, the Nanodyne and Inframat powder lots were found to contain WC particles which ranged from the nanometer scale to the sub-micron scale.

As mentioned above, WC-Co powders were obtained from Nanodyne because they are the only commercial supplier of WC-Co powder containing nanometer-sized WC, as they hold the patent rights on the production of nanometer-sized WC. OGI had expected that all Nanodyne (derived) powders would contain WC particles in the 20 to 100 nanometer range.

Detailed analysis of multiple Nanodyne lots indicates that only one out of the five lots assessed contained nanometer-sized particles in the 20 to 100 nanometer range, as expected. The other four lots contained sub-micron-sized particles, see Table 3.

It is OGI's understanding that the major difference between Nanodyne powder Lots N-1 through N-5 and Lot N-6 was that the first five Nanodyne lots were produced in their pilot plant operation while the N-6 lot was produced in their high-volume production lot facility. It was originally thought that the production facility difference would affect the WC particle size as well as the over-all spray particle interior structure, as the N-6 Lot, produced by the high-volume production facility was the first lot investigated by OGI and was found to contain sub-micron WC particles in porous , but quasi-fully dense, spray particles versus exhibiting a thin/thick shell walls, as expected to be exhibited in the pilot plant powders. However, further study of the various pilot plant lots indicated that selected lots contained sub-micron-sized particles as well as porous, quasi-fully dense spray particles. Thus multiple other high-volume

production lots would need to be assessed before one could make a blanket statement about WC particle size and internal structure of spray particles expected from this production facility.

The Inframat reconstituted Nanodyne powder was also expected to contain nanometer-sized WC particles, as this was suppose to be a way to generate sprayable powder that contained nanometer-sized WC particles. However, this powder was found to contain sub-micron-sized WC. It is not known if this was because the starting Nanodyne powder stock re-constituted by Inframat originally contained sub-micron-sized WC particles or whether the WC particles grew during particle re-constitution. Assessment of the initial feedstock would be needed to answer this question.

CONCLUSIONS

A WC-Co powder needs certain characteristics to be usable as a thermal spray powder. Two of these characteristics are a narrow powder particle size range and flowability. These properties were exhibited by the Sulzer-Metco Powders and the Osram-Sylvania powder. None of the original powder lots furnished by Nanodyne or the lot furnished by Inframat exhibited the narrow range of spray particle sizes and most of the Nanodyne powder lots were found to have poor flowability properties.

A reasonable size range could be achieved by subsequent sizing operations. This sizing operation also resulted in increased flowability, usually by removal of the fines contained in the as-received powder lot. However, increased flowability was not necessarily achieved in the most friable powder lots, as any subsequent "handling" operation resulted in multiple powder particle fracture and re-generation of significant fines. Thus robustness of beginning powder stock is critically important in achieving a thermally sprayable powder. This can be achieved by producing either a thick-walled spray particle or a (substantially) fully dense particle, which may be either porous and/or contain a limited amount of pores.

Expected WC particle sizes were found in the Sultzer-Metco and Osram-Sylvania powders; Sulzer-Metco powder exhibited 1 to 2 μm WC particles while Osram-Sylvania exhibited 200 to 1,200 nanometer (0.2-1.2 μm) particles. Nanodyne powder was found to be the only powder that contained nanometer-scale WC particles (defined as 100 nanometer or less in size), but Nanodyne powder lots were found to vary

significantly in WC particle size. Not all Nanodyne powder lots contained nanometer-scale WC particles; only one out of the five lots analyzed contained nanometer-scale WC particles.

OGI was originally under the impression that all Nanodyne powder lots contained WC particles which varied in size from 20 to 100 nanometers in size. All powder lots were sprayed and reported under this assumption. Recent SEM and TEM analysis of powder from a variety of Nanodyne powder lots has brought this original WC particle size distribution assumption into question. OGI's particle sizing results indicate that only one out of five Nanodyne powder lots received by OGI actually contains (a reasonable) number of WC particles in the 20 to 100 nanometer size range, and that even this powder lot contains WC particles up to 200 nanometers in size. All other Nanodyne powder lots were found to contain (a majority) of sub-micrometer to micrometer-scale WC particles. A Nanodyne re-constituted powder lot recieved from Inframat was also found to contain sub-micrometer WC particles.

The results of this WC particle size indicates that essentially all of the OGI coatings fabricated to date have been done using a sub-micrometer WC particle in a cobalt matrix versus a nanometer-scale WC particles, as originally assumed. Thus the use of the "quote" marks around the nanometer particle size indicators in the above narrative.

OGI finds the results of this study positive even with the materials assesment problems associcated with poor powder flow and lack of nanometer-scale WC particles. The results for the reasonable-quality coatings containing nanometer-to-submicrometer WC-Co particles were, in general, better, to much better than those for the comparison coatings containing micrometer-scale WC-Co particles, in terms of dry-sand-rubber-wheel abrasion tests, coating porosity and coating surface quality. It is expected that use of a "true" WC-Co powder with a true nanometer-scale WC particles may well exhibit increased coating wear and quality properties over those seen for the coatings containing submicrometer-scale WC particles.

Table I. OGI-Received WC-Co powders for use as thermal spray powders

Lot No.	Heat Number	Supplier	Date Received	Wt% Co
SM-1		Sulzer Metco	Spring 98	12
SM-2		Sulzer Metco	Spring 98	17
SM-3	W54785	Sulzer Metco	Summer99	12
N-1		Nanodyne	Fall 97	12
N-2	FP95LR034-1	Nanodyne	Spring 98	15[A]
N-3	FP97LR047	Nanodyne	Spring 98	6
N-4	FP98LR021-1	Nanodyne	Summer 98	15[B]
N-5	FP97LR046-3	Nanodyne	Summer 98	5
N-6a	FP99LR017	Nanodyne	Spring 99	12
N-6b	FP99LR017	Nanodyne	Summer 99	12
I-1	MC101085	Inframat	Summer 99	8
OS-1		Osram-Sylvania	Summer 99	18

Table II. Thermal spray powder characteristics

Lot No. [wt.% Co]	Size Range, (micrometers)	Average Diameter (micrometers)	Fines Quantity	Powder Flow	Spray Particle Structure, see note at end of table
SM-1 [12%Co]	8 to 110	30.4	None	Easy	1
SM-2 [17%Co]	9 to 140	34.8	None	Easy	1
SM-3 [12%Co]	10 to 70	--	None	Easy	1
N-1 [12%Co]	0.8 to 205	26.5	Few	Moderate	Thick-walled Spheres
N-2 [15%Co]	10 to 100	--	Many	Poor	Mostly 1 also 2, 3, 6
N-3 [6%Co]	50 to 300	--	Many	Poor	2, 3, 6, 5
N-4 [15%Co]	5 to 300	--	Many	Poor	5, 3
N-5 [5%Co]	5 to 200	--	Almost all	Poor	2
N-6a [12%Co]	20 to 110	--	Few	Easy	Mostly 5 also 2, 3, 4, 6
N-6b [12%Co]	10 to 50	--	Few	Easy	Mostly 5 also 2, 3, 4, 6
I-1 [8%Co]	2 to 20	--	None	Easy	5
OS-1 [18%Co]	10 to 70	--	None	Easy	1

Notes:

1. Solid spheres
2. Thin-walled spheres
3. Thick-walled spheres
4. Multi-layered spheres;
5. Porous spheres
6. Thin/thick-walled spheres fill with small particles or debris.

Table III. WC Particles Within to the Powder Particles.

Batch No.	WC Particle Size Range (nanometers)	Wt% Co
Micrometer- scale WC Particles		
SM-3	1,000 to 2,000	12
Submicrometer-scale WC Particles		
N-2	200 to 500	15
N-3	200 to 1,000	6
N-5	200 to 1,500	5
N-6	300 to 500	12
I-1	100 to 300	8
OS-1	200 to1,200	18
Nanometer-scale WC Particles		
N-4	20 to 100	15

(a)

(b)

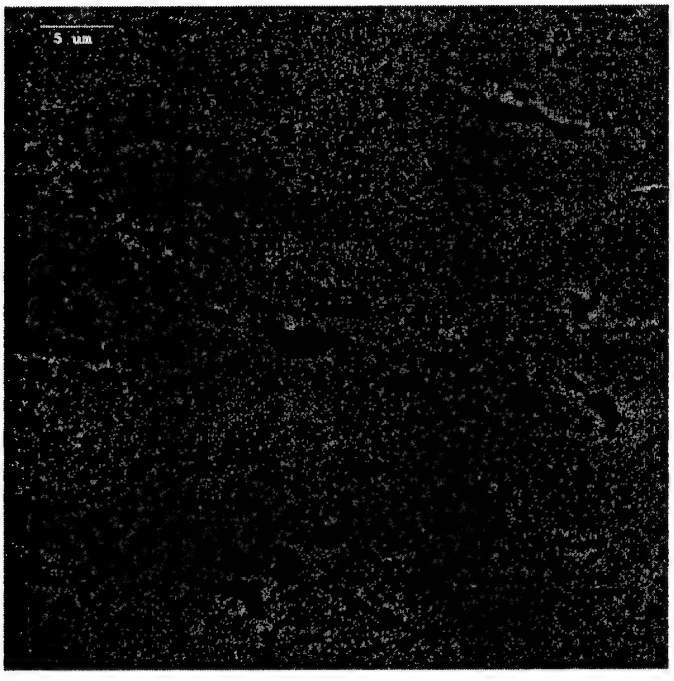

Figure 1. Photomicrographs of WC-Co coating with submicrometer (near nanometer scale) WC in secondary electron imaging (a) and backscattered imaging mode (b).

(a)

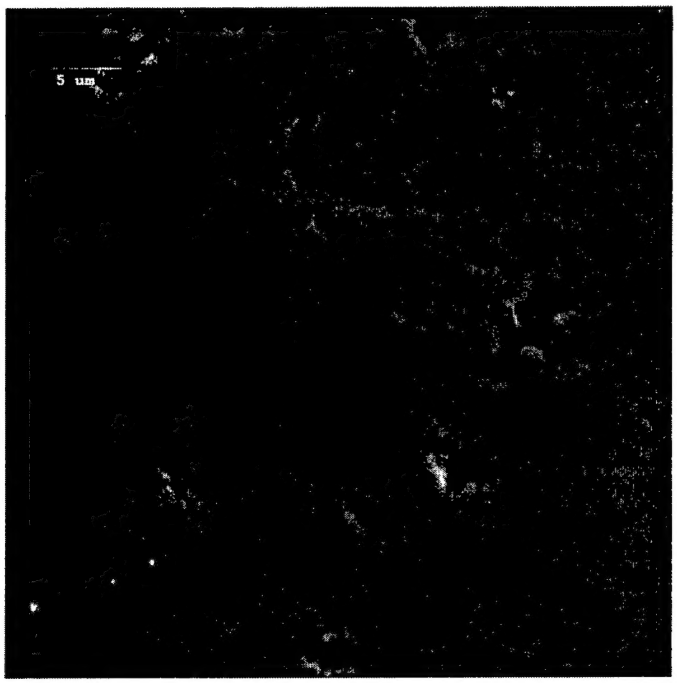

(b)

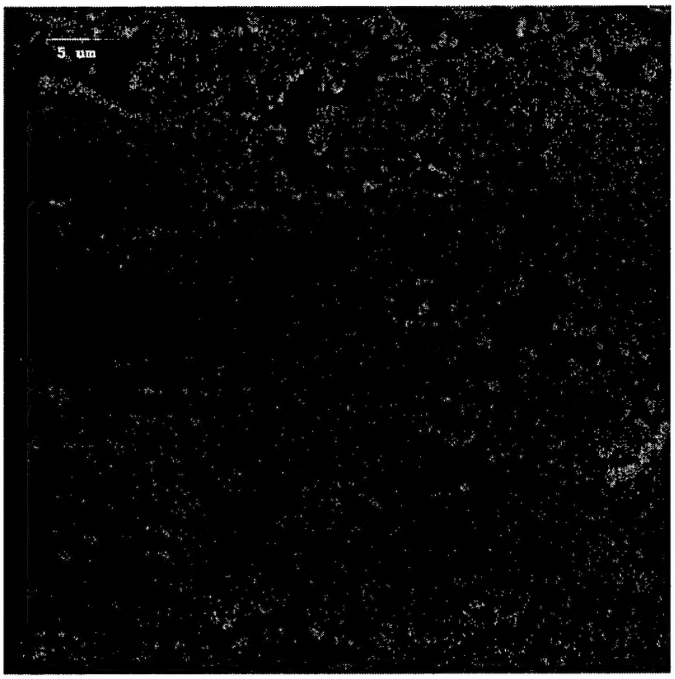

Figure 2. Photomicrographs of WC-Co coating with micrometer WC in secondary electron imaging (a) and backscattered imaging mode (b).

(a)

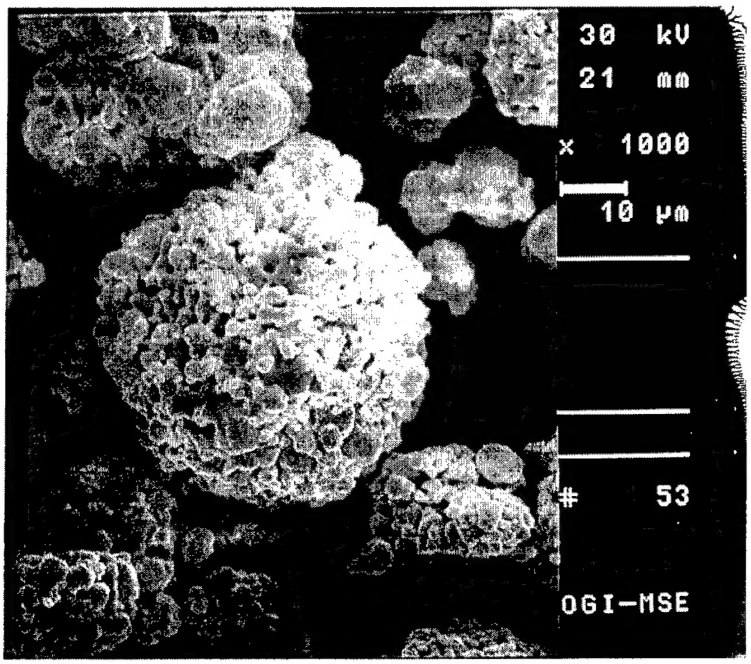

(b)

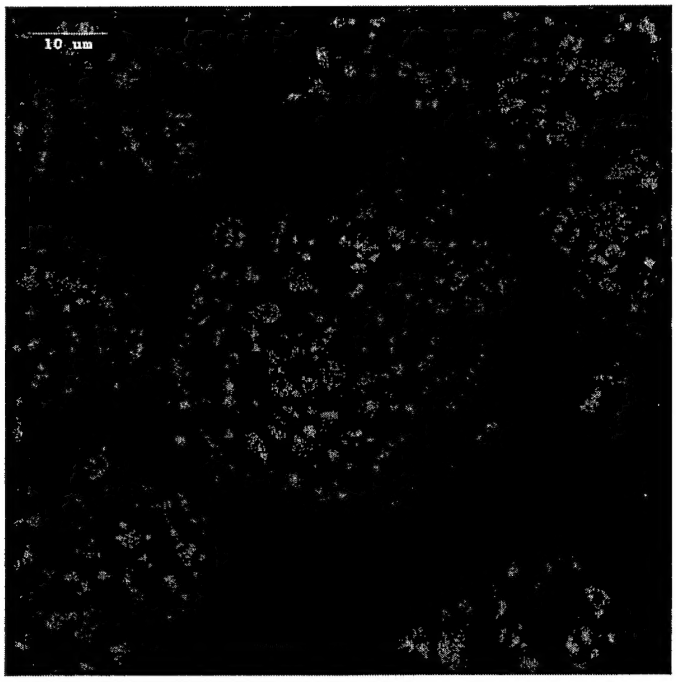

Figure 3. Photographs of conventional WC-Co thermal spray powder with micrometer scale WC in secondary electron imaging (a) and backscattered electron imaging mode (b).

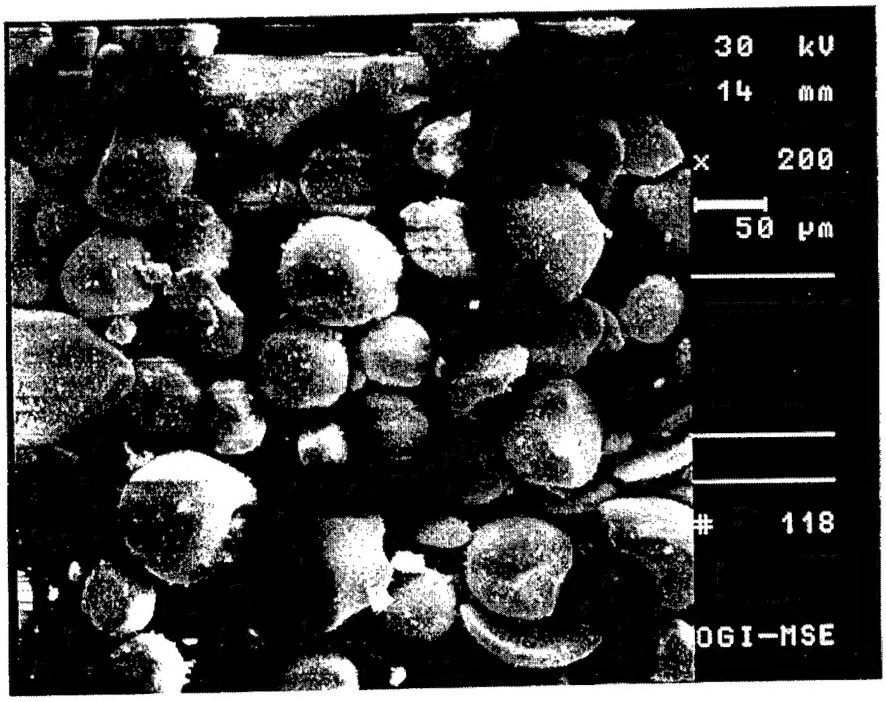

Figure 4. Photograph of 'good' WC-Co thermal spray powder with nanometer scale WC in secondary electron imaging.

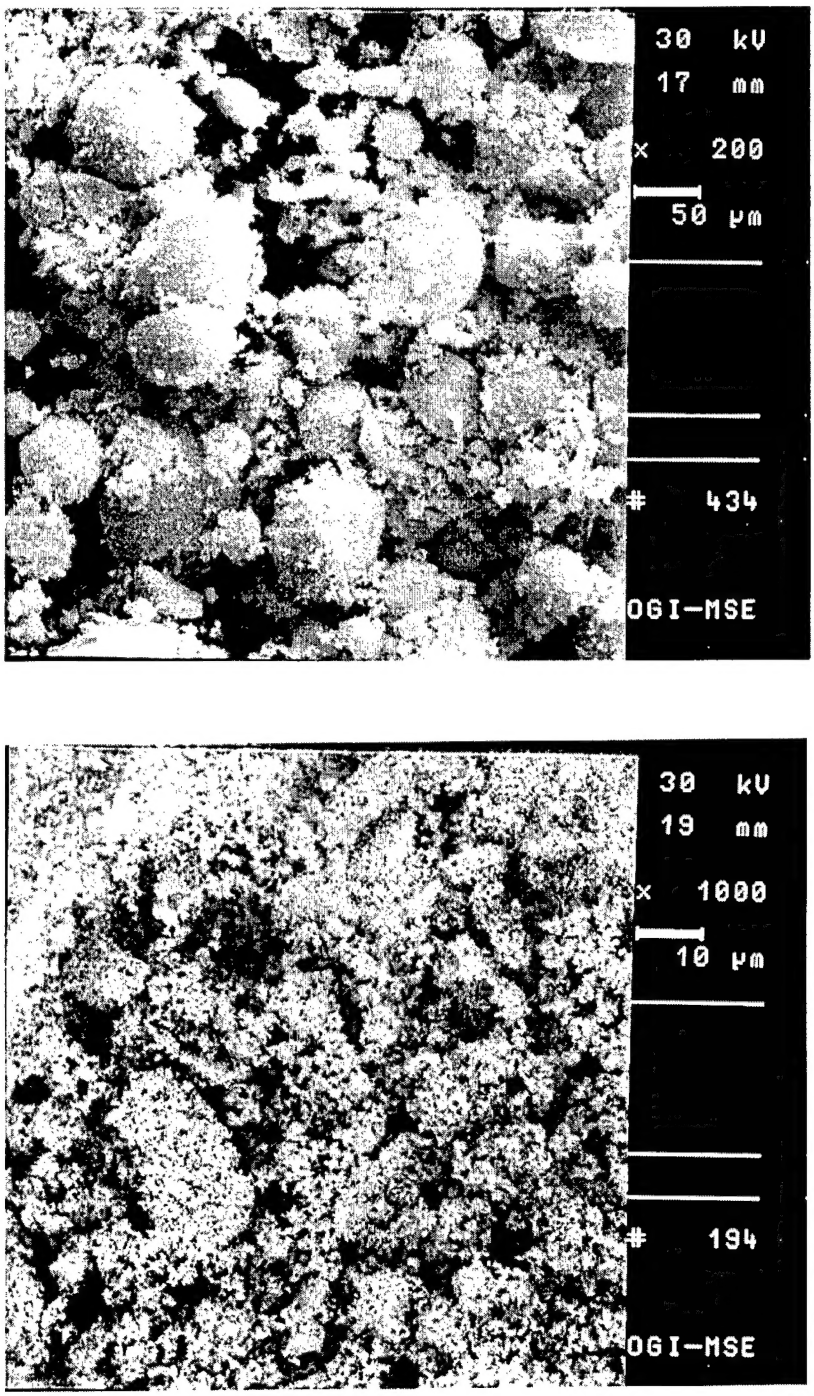

Figure 5. Photograph of 'poor' WC-Co thermal spray powder with nanometer scale WC in secondary electron imaging.